Analysis of Dielectric *E*-Plane Waveguides and Design of Filters

Hiroshi Kubo, *Member, IEEE,* Hiroshi Yamashita, *Associate Member, IEEE,* and Ikuo Awai, *Member, IEEE*

***Abstract*— A small-size waveguide made of high-permittivity ceramic is analyzed. The propagation constants are calculated approximately by an approach where the electromagnetic fields outside the waveguide are fully taken into consideration. The analysis values agree well with the experimental values. The constants of equivalent circuit for the metallic strip section are obtained by using a separate model for the analysis of the structure. Based on these results, bandpass filters (BPF's) are designed and fabricated. The fabricated BPF's have better transmission and reflection characteristics than those designed on the basis of a trough-guide model.**

***Index Terms*— Dielectric waveguide, electromagnetic analysis, filters, waveguide filters.**

I. Introduction

RECENTLY, there has been much interest in the miniaturization of microwave passive components because of the need for a small and lightweight handset for mobile communications [1]. Dielectric ceramic of high permittivity has the effect of wavelength shortening. Small-size bandpass filters (BPF's) for lower microwave frequency bands based on dielectric waveguide [2] have been developed in this way.

The present waveguide structure is a half-cut of a rectangular metal waveguide filled with high-permittivity ceramic [3], which will be referred to as a dielectric E-plane waveguide (DEW). The high permittivity ceramic (relative permittivity $\varepsilon_c = 83$) makes the component size small. The open surface created is convenient for attaching some metallic strip patterns, resulting in a quasi-finline structure.

Analysis data for the propagation characteristics is necessary to design the resonator sections and the coupling sections of DEW filters. Approximate approaches may be effectively applied to the analysis because the field energy is confined in the waveguide and the energy leaking out of the open surface is small due to the high permittivity. The modified waveguide structure with assumed electric walls on the top and bottom surfaces has been analyzed and BPF's have been designed [4]. The center frequency of the fabricated filters agreed with the designed values, but the bandwidth did not give good agreement and the return loss was poor.

In this paper, we analyze a DEW in full consideration of the field expanding outside the open surface. The propagation constants obtained are compared with the experimental values. Then, on the basis of the propagation constants and the analysis results of the coupling coefficients in the modified structure, several BPF's are designed and fabricated.

Manuscript received April 24, 1997; revised May 11, 1998.

The authors are with the Department of Electrical and Electronic Engineering, Yamaguchi University, Tokiwadai, Ube-shi 755, Japan.

Publisher Item Identifier S 0018-9480(98)05512-4.

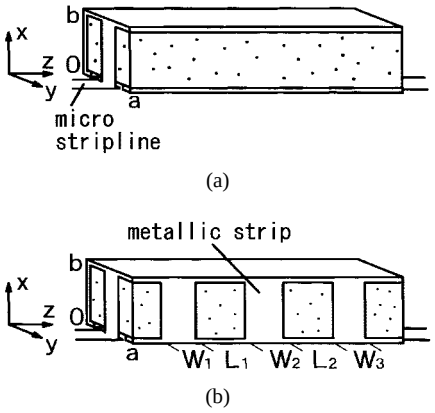

Fig. 1. (a) Basic structure of DEW. (b) Structure of a DEW BPF.

II. Analysis

Fig. 1(a) shows the basic structure of a DEW. The waveguide is made of high-permittivity ceramics and the side faces (except one) are coated with metal. Although one side face is exposed to the outer region, the high-permittivity ceramic effectively confines the electromagnetic fields in the waveguide. By forming some metallic strip patterns on the open surface, the waveguide is divided into several resonator sections between cutoff sections. The coupling between two adjacent resonators can be adjusted by the width of the strip. Thus, we can make a multistage filter with a tandem connection of waveguide resonators. Fig. 1(b) shows a two-stage DEW filter. W_i: $(i = 1,2,3)$ and L_j: $(j = 1,2)$ denote the width of strips and the length of resonator sections, respectively.

A. Phase Constant

We analyze the propagation characteristics of a basic DEW. For simplifying the analysis, we assume two hypothetical electric walls. Fig. 2 shows the cross section of a DEW with the assumed two electric walls on the planes $x \geq b, y = a$ and $x \leq 0, y = a$. It is expected that the presence of these walls do not have much influence on the result because the greater part of field energy is confined in the waveguide with high permittivity. S_c denotes the ceramic region of the waveguide and S_e denotes the exterior air region $y > a$. The guided waves are assumed to vary in the form of $\exp(-j\beta z)$, where β is a real phase constant in the z-direction. The field of the

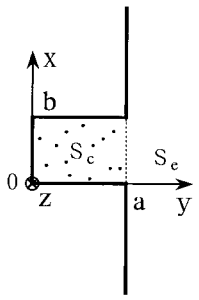

Fig. 2. Cross section of a DEW with two assumed electric walls on the planes $x \geq b, y = a$ and $x \leq 0, y = a$.

dominant mode is TE_{10}-like in S_c and the electric-field lines expand in the $\pm x$-directions in S_e. We formulate the fields on the following two assumptions: E_y, which is not zero in S_e, is approximated as $E_y \equiv 0$ in S_c, taking account of the continuity of electric-flux density component normal to the open surface and the high permittivity of S_c and $E_z \equiv 0$ in both S_c and S_e. This is a fairly good approximation in S_c and may be a rough approximation in S_e. Thus, in S_c, the electric field has only an x-component and the electromagnetic field has no dependence on x.

First, the impedance Z_c on the open surface looking inward is deduced as follows:

$$Z_c = Z_{cy} \tan(k_{cy} a) \tag{1}$$

where

$$Z_{cy} = \frac{j\omega\mu}{k_{cy}} \tag{2}$$

$$k_{cy} = \sqrt{\varepsilon_c k_0^2 - \beta^2} \tag{3}$$

Z_{cy} is the wave impedance in the $-y$-direction in S_c, μ is a permeability that is common in two regions, ε_c is the relative permittivity in S_c, and k_0 is the wavenumber in free space.

Secondly, we derive the impedance Z_e on the open surface looking outward. The fields in S_c can be represented by

$$E_{cx} = \frac{A}{1+\Gamma_y} \Big[\exp\{-jk_{cy}(y-a)\} + \Gamma_y \exp\{jk_{cy}(y-a)\}\Big] \exp(-j\beta z) \tag{4}$$

$$H_{cz} = \frac{\omega\mu}{k_{cy}} \frac{A}{1+\Gamma_y} \Big[-\exp\{-jk_{cy}(y-a)\} + \Gamma_y \exp\{jk_{cy}(y-a)\}\Big] \exp(-j\beta z) \tag{5}$$

where A and Γ_y are the amplitude and reflection coefficient of E_{cx} at $y = a$, respectively. Using (4) and (5), the complex power flow P_c into the open surface out of S_c per unit length to the z-direction is given by

$$P_c = -\int_0^b [E_{cx} H_{cz}^*]_{y=a}\, dx = b|A|^2 \frac{1-\Gamma_y^*}{1+\Gamma_y^*} \frac{k_{cy}}{\omega\mu} \tag{6}$$

where the asterisk means the complex conjugate of the indicated symbol.

We represent the fields in S_e by the z-component Φ_e of a magnetic vector potential. Φ_e is given by

$$\Phi_e = \frac{j\omega\mu}{2\pi(k_0^2 - \beta^2)} \int_{-\infty}^{\infty} f(k_{ex}) \exp(-jk_{ex}x) \cdot \exp\{-jk_{ey}(y-a)\} \exp(-j\beta z)\, dk_{ex} \tag{7}$$

$$k_{ey} = -j\sqrt{\beta^2 - k_0^2 + k_{ex}^2}, \tag{8}$$

where k_{ex} denotes the wavenumber in the x-direction. Using the Fourier transform of Φ_e with respect to x, we obtain

$$\overline{E}_{ex} = \frac{\omega\mu k_{ey}}{\beta^2 - k_0^2} f(k_{ex}) \exp\{-jk_{ey}(y-a)\} \exp(-j\beta z) \tag{9}$$

$$\overline{H}_{ez} = \frac{\beta^2 - k_0^2}{\omega\mu k_{ey}} \overline{E}_{ex} \tag{10}$$

where a bar over a symbol denotes a Fourier transform. Considering $E_{ex} = A$ on the open surface $(0 \leq x \leq b)$, $\overline{E}_{ex}$ at $y = a$ is obtained as follows:

$$\overline{E}_{ex}|_{y=a} = \int_{-\infty}^{\infty} E_{ex}(x, a, z) \exp(jk_{ex}x)\, dx = 2A \exp(jk_{ex}b/2) \frac{\sin k_{ex}b/2}{k_{ex}} \exp(-j\beta z). \tag{11}$$

Using (10) and (11), the complex power flow P_e into S_e out of the open surface is given by

$$P_e = -\int_{-\infty}^{\infty} [E_{ex} H_{ez}^*]_{y=a} dx = -\frac{1}{2\pi} \int_{-\infty}^{\infty} [\overline{E}_{ex} \overline{H}_{ez}^*]_{y=a}\, dk_{ex} = -\frac{2(\beta^2 - k_0^2)}{\pi\omega\mu} \left|A\right|^2 \int_{-\infty}^{\infty} \frac{\sin^2(k_{ex}b/2)}{k_{ey}^* k_{ex}^2}\, dk_{ex}. \tag{12}$$

On the open surface, the relation $P_c = P_e$ applies. Substitution of (6) and (12) into the relation and some transformations give

$$\frac{1+\Gamma_y}{1-\Gamma_y} \frac{\omega\mu}{k_{cy}} = \frac{j\omega\mu\pi}{b(\beta^2 - k_0^2)} \cdot \left(\int_0^{\infty} \frac{\sin^2 v}{v^2 \sqrt{(\beta^2 - k_0^2)(b/2)^2 + v^2}}\, dv \right)^{-1} \tag{13}$$

where

$$v = k_{ex} b/2. \tag{14}$$

The left-hand side of (13) represents Z_e. Since the guided mode field satisfies the relation $Z_c^* = Z_e$, we obtain

$$\frac{\tan(\sqrt{\varepsilon_c k_0^2 - \beta^2}\, a)}{\sqrt{\varepsilon_c k_0^2 - \beta^2}} = \frac{\pi}{b(\beta^2 - k_0^2)} \left(\int_0^{\infty} \frac{\sin^2 v}{v^2 \sqrt{(\beta^2 - k_0^2)(b/2)^2 + v^2}}\, dv \right)^{-1}. \tag{15}$$

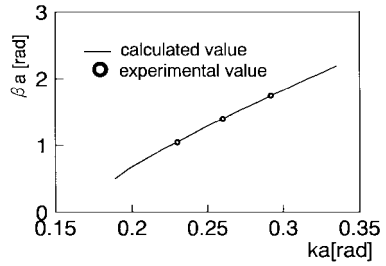

Fig. 3. Calculated (—) and experimental (o) dispersion relations of the waveguide with $a = 5$ mm, $b = 3$ mm, and $\varepsilon_c = 83$.

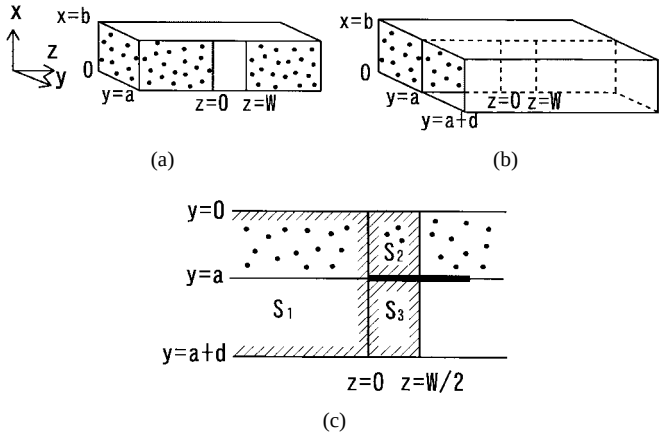

Fig. 4. Schematic structure of strip section. (a) Strip section of DEW. (b) Strip section of DEW with two electric walls placed on $x = 0$ and b planes and one electric wall on $y = a + d$ plane. (c) Cross-sectional view of (b).

The dispersion relations can be obtained by numerically solving (15).

Fig. 3 shows the dispersion relation of the waveguide with $a = 5$ mm, $b = 3$ mm, and $\varepsilon_c = 83$. The analysis results of (15) are plotted by the solid line. The experimental results are plotted as the three small circles. The experimental values were obtained by measuring the resonant frequencies of the DEW with large copper sheets pasted on both end faces with respect to the z-direction. The analysis results agree well with the experimental values.

B. Coupling Coefficient

The coupling coefficients between resonator sections are required to design filters. The metallic strip sections in Fig. 4(a) having a three-dimensional structure can be precisely analyzed only by using a large-scale computer. We substitute the coupling coefficients of the strip section in Fig. 4(b) for those in Fig. 4(a). In Fig. 4(b), we assume two electric walls placed on $x = 0$ and b planes and one electric wall on $y = a + d$ plane sufficiently apart from the open surface.

If we choose terminal reference planes at $z = 0$ and W, the equivalent circuit for the strip section is represented by the T network in Fig. 5 and jX_s and jX_p are given by [5]

$$jX_s = \frac{1}{X^e}$$
$$jX_p = \frac{1}{2}\left(\frac{1}{X^m} - \frac{1}{X^e}\right) \tag{16}$$

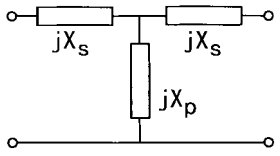

Fig. 5. Equivalent T network of the strip section.

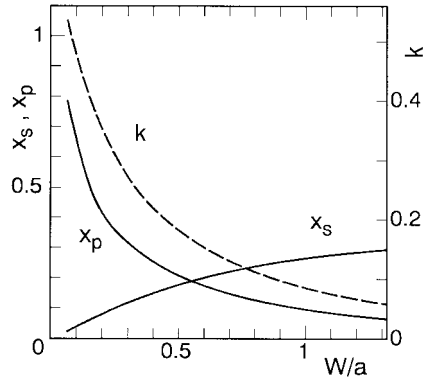

Fig. 6. Calculated values of normalized series reactance x_s, shunt reactance x_p, and coupling coefficient k of strip section in Fig. 4(b) with $a = 5$ mm, $b = 3$mm, $d = 50$ mm, and $\varepsilon_c = 83$ for $f = 2.5$ GHz.

where X^e and X^m denote the input impedance to the strip section with an electric and a magnetic wall at the $z = W/2$ plane, respectively. Let a dominant mode (TE_{10}-like) be incident on the strip section from the $-z$-direction. X^p $(p = e, m)$ for the incident wave are calculated at first. We consider three regions S_1 $(z < 0)$, S_2 $(0 < z < W/2$ inside the dielectric) and S_3 $(0 < z < W/2$ outside the dielectric), shown in Fig. 4(c). The fields $E^p_{\ell x}$ $(\ell = 1, 2, 3)$ in these regions are represented in (17)–(24), shown at the bottom of the following page, and Γ is the reflection coefficient for the dominant mode $(n = 1)$ at $z = 0$, and $\kappa_{1c,n}$, $\kappa_{1e,n}$, and $\beta_{1,n}$ satisfy the relations

$$\beta^2_{1,n} = \varepsilon_c k_0^2 - \kappa^2_{1c,n} = k_0^2 - \kappa^2_{1e,n} \tag{25}$$
$$\kappa_{1c,n} \tan \kappa_{1e,n} d = -\kappa_{1e,n} \tan \kappa_{1c,n} a \tag{26}$$

where

$\kappa_{1c,n}$ positive real, $\kappa_{1c,1} < \kappa_{1c,2} < \kappa_{1c,3} < \cdots$

$\kappa_{1e,n}, \beta_{1,n}$ positive real or negative imaginary.

$H^p_{\ell y}$ is given by $E^p_{\ell x}$ through the relation

$$H^p_{\ell y} = \frac{j}{\omega\mu}\frac{\partial}{\partial z} E^p_{\ell x}. \tag{27}$$

Matching these fields at the boundary $z = 0$ in the mean square sense [6], [7], the unknown expansion coefficients $C^p_{\ell,n}$ can be determined. Substituting these fields into the relation at the boundary [8]

$$\int_0^{a+d} E^p_{1x} H^{p*}_{1y}\, dy = \int_0^{a} E^p_{2x} H^{p*}_{2y}\, dy + \int_a^{a+d} E^p_{3x} H^{p*}_{3y}\, dy \tag{28}$$

we obtain the normalized impedance of (29), shown at the bottom of the following page.

Using these equations, we calculate x^e and x^m for the strip section in DEW with

$$a = 5 \text{ mm} \quad b = 3 \text{ mm} \quad \varepsilon_c = 83$$

for a frequency $f = 2.5$ GHz. After confirming the convergency of the numerical solutions, the position of an electric wall d is chosen as $d = 50$ mm and the truncation number N is chosen as $N = 100$. In Fig. 6, the calculated values for the normalized series reactance x_s and the normalized shunt reactance x_p are plotted by the solid lines.

III. Design and Fabrication of BPF

We use the design method for n-stage BPF's according to the following relations [9], [10]:

$$\phi_i = -\tan^{-1}(2x_{pi} + x_{si}) - \tan^{-1} x_{si} \tag{30}$$

$$k_{i-1,i} = |\tan(\phi_i/2 + \tan^{-1} x_{si})|, \qquad i = 1, 2, \cdots, n+1 \tag{31}$$

$$L_j = \frac{1}{\beta}\left(\pi + \frac{\phi_j + \phi_{j+1}}{2}\right), \qquad j = 1, 2, \cdots, n \tag{32}$$

$$k_{0,1} = \left(\frac{\eta w}{g_0 g_1}\right)^{1/2}$$

$$k_{n,n+1} = \left(\frac{\eta w}{g_n g_{n+1}}\right)^{1/2}$$

$$k_{i-1,i} = w\eta\left(\frac{1}{g_{i-1} g_i}\right)^{1/2} \tag{33}$$

$$w = \frac{\Delta f}{f_0} \tag{34}$$

$$\eta = \frac{\pi}{2}\,\varepsilon_c\left(\frac{k_0}{\beta}\right)^2 \tag{35}$$

where x_{pi} and x_{si} are the normalized series and shunt reactances of the ith strip, respectively, $k_{i-1,i}$ is the coupling coefficient between both resonator sections adjacent to the ith strip, L_j is the length of the jth resonator section, Δf is the bandwidth of a BPF, f_0 is the center frequency, β is the phase constant calculated in the preceding section, and g_i is the normalized element value of a prototype low-pass filter (LPF). Substituting the values of x_p and x_s of Fig. 6 into (30) and (31), we can calculate k for the strip width W. In Fig. 6, k values for a frequency $f = 2.5$ GHz are plotted by the

---

region S_1:

$$E^p_{1x} = \frac{C^p_{1,1}}{1+\Gamma}\,\{\exp(-j\beta_{1,1}z) + \Gamma\exp(j\beta_{1,1}z)\}e_{1,1}(y) + \sum_{n=2}^{N} C^p_{1,n}\exp(j\beta_{1,n}z)e_{1,n}(y) \tag{17}$$

region S_2, S_3:

$$E^p_{\ell x} = \begin{cases} \displaystyle\sum_{n=1}^{N} C^e_{\ell,n}\sin\beta_{\ell,n}\left(z - \frac{W}{2}\right)e_{\ell,n}(y) & \text{for electric wall} \\ \displaystyle\sum_{n=1}^{N} C^m_{\ell,n}\cos\beta_{\ell,n}\left(z - \frac{W}{2}\right)e_{\ell,n}(y) & \text{for magnetic wall} \end{cases}, \qquad \ell = 2, 3,\ p = e, m \tag{18}$$

where

$$e_{1,n}(y) = \begin{cases} F_n \sin\kappa_{1c,n}y, & \text{for } 0 \le y \le a \\ F_n\,\dfrac{\sin\kappa_{1c,n}a}{\sin\kappa_{1e,n}d}\,\sin\kappa_{1e,n}(a+d-y), & \text{for } a \le y \le a+d \end{cases} \tag{19}$$

$$e_{2,n}(y) = \sqrt{\frac{2}{a}}\,\sin\frac{n\pi}{a}y \tag{20}$$

$$e_{3,n}(y) = \sqrt{\frac{2}{d}}\sin\frac{n\pi}{d}y \tag{21}$$

$$\frac{1}{F_n} = \sqrt{\frac{a}{2} - \frac{\sin 2\kappa_{1c,n}a}{4\kappa_{1c,n}} + \left(\frac{\sin\kappa_{1c,n}a}{\sin\kappa_{1e,n}d}\right)^2\left(\frac{d}{2} - \frac{\sin 2\kappa_{1e,n}d}{4\kappa_{1e,n}}\right)} \tag{22}$$

$$\beta_{2,n} = -j\sqrt{\left(\frac{n\pi}{a}\right)^2 - \varepsilon_c k_0^2} \tag{23}$$

$$\beta_{3,n} = -j\sqrt{\left(\frac{n\pi}{d}\right)^2 - k_0^2}, \qquad n = 1, 2, 3, \cdots \tag{24}$$

$$x^p = \frac{1+\Gamma}{1-\Gamma} = \beta_{1,1}|C^p_{1,1}|^2 \Bigg/ \left(\sum_{n=2}^{N}\beta_{1,n}|C^p_{1,n}|^2 - \frac{1}{2}\sum_{n=1}^{N} j\beta_{2,n}|C^p_{2,n}|^2\,\sin^* W\beta_{2,n} - \frac{1}{2}\sum_{n=1}^{N} j\beta_{3,n}|C^p_{3,n}|^2\sin^* W\beta_{3,n}\right) \tag{29}$$

TABLE I
STRIP WIDTH W_i AND RESONATOR SECTION LENGTH L_j FOR VARIOUS BPF CHARACTERISTICS WITH $a = 5$ mm, $b = 3$ mm, AND $\varepsilon_c = 83$

DESIGNED VALUE			DIMENSION OF STRIP PATTERNS						
f_0 [GHz]	Δf [MHz]	NUMBER OF STAGES	W_1 [mm]	W_2 [mm]	W_3 [mm]	W_4 [mm]	L_1 [mm]	L_2 [mm]	L_3 [mm]
2.5	50	2	1.59	6.17	1.59		8.55	8.55	
2.5	100	2	0.90	3.57	0.90		8.38	8.38	
2.5	150	2	0.58	2.36	0.58		8.21	8.21	
2.5	100	3	0.62	3.58	3.58	0.62	8.27	8.63	8.27
2.2	100	2	0.37	2.01	0.37		11.3	11.3	
2.8	100	2	1.80	5.53	1.80		6.25	6.25	

TABLE II
DESIGNED VALUES OF BPF CHARACTERISTICS AND EXPERIMENTAL VALUES WITH $a = 5$ mm, $b = 3$ mm, AND $\varepsilon_c = 83$

DESIGNED VALUE			EXPERIMENTAL VALUE				
f_0 [GHz]	Δf [MHz]	NUMBER OF STAGES	f_0 [GHz]	ERROR [%]	Δf [MHz]	ERROR [%]	S_{11} [dB]
2.5	50	2	2.49	-0.4	51.5	2.9	-33
2.5	100	2	2.50	0.0	110.6	10.6	-24
2.5	150	2	2.48	-0.8	171.9	14.6	-20
2.5	100	3	2.45	-2.0	101.8	1.8	-26
2.2	100	2	2.21	0.5	121.0	21.0	-20
2.8	100	2	2.75	-1.8	91.0	-9.0	-41

broken line. W_i can be obtained by calculating $k_{i-1,i}$ in (33) and referring to Fig. 6. It must be noted that k values depend on β through (34) and (35). L_j can be determined by (32).

We have designed a two-stage Butterworth BPF with $f_0 = 2.5$ GHz and bandwidth $\Delta f = 50$ MHz. Metallic strip patterns are formed on the open surface of a DEW with width $a = 5$ mm, height $b = 3$ mm, and relative permittivity $\varepsilon_c = 83$. The strip width W_i and resonator section length L_j are as follows:

$$W_1 = W_3 = 1.59 \text{ mm}$$
$$W_2 = 6.17 \text{ mm}$$
$$L_1 = L_2 = 8.55 \text{ mm}.$$

Fig. 7 shows the transmission and reflection characteristics of the experimental filter. After confirming a considerable agreement between the design and experimental results, we have designed and fabricated various BPF's. The designed values of BPF's characteristics and the dimension of strip patterns are shown in Table I, and the experimental values are shown in Table II. The center frequencies of the fabricated BPF's agree well with the prediction. Some fabricated BPF's have bandwidths equal to the designed values, and others have bandwidths considerably different from the design. The disagreement can be seen especially in the wide-band types and a low center-frequency type. These types of filters have short strip sections, which cause strong coupling between resonators. In the strong coupling region, it can be concluded that the theory is in error.

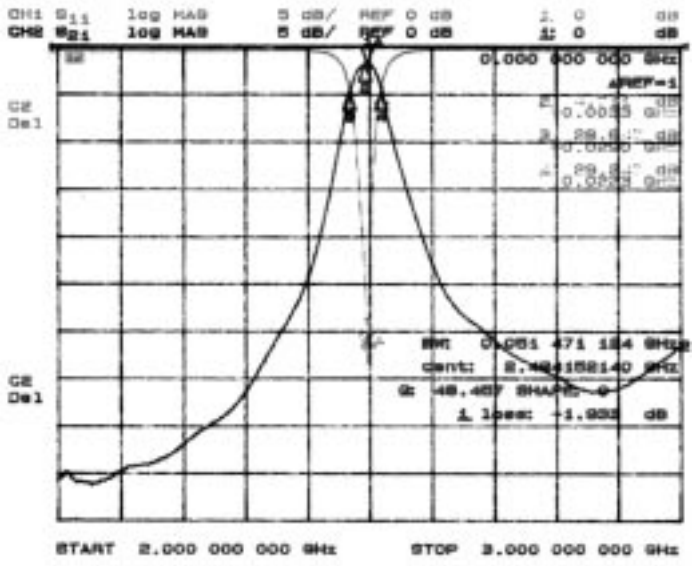

Fig. 7. Transmission and reflection characteristics of fabricated filter with $f_0 = 2.5$ GHz, bandwidth $\Delta f = 50$ MHz, $a = 5$ mm, $b = 3$ mm, $\varepsilon_c = 83$.

Finally, we touch on the open surface. Besides conductor loss and dielectric loss, there is radiation loss, which has not been analytically evaluated. The conductors more than 2 cm

apart from the open surface does not affect the characteristics of filters.

IV. Conclusion

Dielectric E-plane waveguides have been analyzed with full consideration of the outside field distribution, and the dispersion relation has been presented. Close agreement between calculated and experimental values was obtained. We have also calculated the coupling coefficients of E-plane strips of the waveguide with assumed electric walls. Using these results, BPF's have been designed and fabricated. The center frequencies of the fabricated BPF's agree well with the designed values. Though the experimental bandwidth values are improved to some extent, compared with the previous results [4], the errors are still not small in the cases of wide bandwidths and low center frequencies. It should also be added that all the numerical analyses in this paper do not require a large-scale computer and can easily be carried out on a personal computer.

Acknowledgment

The authors thank R. Kitou and S. Furuya of Ube Industries, Ltd., Ube-shi, Japan, for providing them with the ceramic materials and Prof. M. Hano and A. Kirihara of Yamaguchi University, Ube-shi, Japan, for their helpful advice.

References

[1] T. Nishikawa, "Front end circuit components miniaturized using dielectric resonators for cellular portable telephones," *IEICE Trans.*, vol. E74, pp. 1556–1562, June 1991.

[2] M. Hano, S. Furuya, and I. Awai, "Three-dimensional finite element analysis of dielectric E-plane waveguide filters," in *Proc. APMC'92*, Adelaide, Australia, Aug. 1992, pp. 441–444.

[3] Y. Konishi, K. Konno, and I. Awai, "Novel dielectric-waveguide components," *IEEE Trans. Broadcast.*, vol. 34, pp. 2–8, Mar. 1988.

[4] H. Kubo, I. Awai, K. Yamaguchi, and M. Hano, "Design and fabrication of bandpass filters based on a dielectric E-plane waveguide," in *IEEE MTT-S Int. Microwave Symp. Dig.*, vol. 1, San Diego, CA, May 23–27, 1994, pp. 241–244.

[5] R. E. Collin, *Field Theory of Guided Waves*. New York: McGraw-Hill, 1960, ch. 8.

[6] K. Yasuura, "A view of numerical methods in diffraction problems," in *Progress in Radio Science 1966–1969*, W. V. Tilson and M. Sauzade, Eds. Brussels, Belgium: URSI, 1971, pp. 257–270.

[7] H. Kubo and K. Yasumoto, "Numerical analysis of cylindrical dielectric waveguide with periodically varying radius," *IEICE Trans. Electron.*, vol. E74-C, pp. 384–390, Feb. 1991.

[8] R. F. Harrington, *Time-Harmonic Electromagnetic Fields*. New York: McGraw-Hill, 1961, ch. 8.

[9] Y. Konishi and K. Uenakada, "The design of a bandpass filter with inductive strip-planar circuit mounted in waveguide," *IEEE Trans. Microwave Theory Tech.*, vol. MTT-22, pp. 869–873, Oct. 1974.

[10] Y. C. Shih, "Design of waveguide E-Plane filters with all-metal inserts," *IEEE Trans. Microwave Theory Tech.*, vol. MTT-32, pp. 695–704, July 1984.

Hiroshi Kubo (M'92) received the B.E., M.E., and D.E. degrees from Kyushu University, Fukuoka, Japan, in 1978, 1980, and 1993, respectively.

From 1980 to 1985, he was with the Nippon Electric Company, Tokyo, Japan, where he was engaged in development on mobile communication system. From 1985 to 1987, he worked as a Development Engineer at the Kyushu Matsushita Electric Company, Fukuoka, Japan. From 1987 to 1991, he was a Research Associate at Kyushu University. Since 1991, he has been with Yamaguchi University, Ube-shi, Japan, where he is currently an Associate Professor. His main area of research interest is dielectric waveguides and waveguide components.

Hiroshi Yamashita (A'85) received the B. Eng. degree from Yamaguchi University, Ube-shi, Japan, in 1995.

Since 1995, he has been with the Kansai Heat Chemical Company, Kakogawa, Japan.

Ikuo Awai (M'78) received the B.S., M.S., and the Ph.D. degrees from Kyoto University, Kyoto, Japan, in 1963, 1965, and 1978, respectively.

In 1968, he joined the Department of Electronics, Kyoto University, as a Research Associate, where he was engaged in research on microwave magnetic waves and integrated optics. From 1984 to 1990, he worked for the Uniden Corporation, Tokyo, Japan, where he developed microwave communication equipments. In 1990, he joined Yamaguchi University, Ube-shi, Japan, where he is currently a Professor. His research interests include the study of magnetostatic wave devices, dielectric waveguide components, and superconducting devices for microwave application.